Heliyon 6 (2020) e04019

Contents lists available at ScienceDirect

Heliyon

journal homepage: www.cell.com/heliyon

Research article

Biochar production from palm oil mill residues and application of the biochar to adsorb carbon dioxide

Archw Promraksa [a,b], Nirattisai Rakmak [a,b,*]

[a] Biomass and Oil-Palm Excellence Center, Thailand
[b] School of Engineering and Technology, Walailak University, Thailand

ARTICLE INFO

Keywords:
Chemical engineering
Environmental chemical engineering
Materials characterization
Adsorption
Biochar
Pyrolysis
Palm oil
CO_2
RSM

ABSTRACT

The amount of palm oil mill residues increases rapidly and will become a severe problem in the future. One potential technique for alleviating this concerning environmental problem is to convert these residues into biochar by the pyrolysis process. Pyrolysis of three types of palm oil mill residues (namely, palm kernel shells, empty palm fruit bunches, and oil palm fibers) was conducted in a fixed bed reactor at 500 °C and 2 L/min of nitrogen flow rate for 60 min. The optimization of biochar production was performed using the Box-Behnken design and analyzed using response surface methodology. The effects of three potential factors, including pyrolysis temperatures, nitrogen flow rates, and biomass particle sizes, were studied. The results showed that the highest biochar yield (44.91 wt%) was obtained from pyrolysis of palm kernel shells at 525 °C with a nitrogen flow rate of 2 L/min and a particle size of 750 μm. Application of biochar produced from palm kernel shells for carbon dioxide capture was tested in a packed bed adsorber of 3.0 g of biochar sample by flowing 1,400 ppm of carbon dioxide in the gas feed mixture at 2.5 L/min. The capacity of the biochar sample for CO_2 adsorption was 0.46 mmol/g.

1. Introduction

Palm oil production is one of the primary industries in Southern Thailand. Nowadays, palm oil mill residues: mainly empty palm fruit bunches, oil palm fibers, and palm kernel shells have been massively generated [1]. Moreover, this plant generates significant amounts of liquid waste. Palm oil mill effluents from the palm oil production process can be utilized not only as animal feedstocks or fertilizers but also in electricity by converting them into biogas. In palm oil mills, these residues are generally sent to the boiler for burning as fuel for steam generation or used for the reduction of energy (diesel or electricity) consumption. However, this process is not environmentally friendly because it produces smoke and dust emissions due to incomplete combustion. The biomass residues from palm oil processing could be potentially used as a renewable energy source by conversion into biofuel or other bio-products. The use of biomass in other forms of energy products is more beneficial than the direct burning of biomass because it does not release any pollutants into the air. One potential technique for alleviating these environmental concerns is to convert palm oil residues into biochar by the pyrolysis process. Pyrolysis is an anaerobic process of the thermal decomposition of the chemical structure of organic material at a high temperature, and the products of this process are biochar, bio-oil, and syngas [2].

The emissions of carbon dioxide (CO_2) into the atmosphere have been a critical concern because they could induce more climate change. CO_2 contributes to the most significant amount of gases among greenhouse gases. Power plants are a primary industrial source of CO_2 emissions since they consume a massive amount of fossil fuels to generate energy for human activities and usages. Additionally, CO_2 is an acid gas that can cause acid rain and corrosion of pipes or containers used in transportation and storage systems. To minimize the release of CO_2 into the atmosphere, many researchers have earnestly attempted to find novel and modern ways to use technology and high potential materials to capture CO_2 effectively. For the industrial process, CO_2 as natural gas can be absorbed in the solution of monoethanolamine (MEA), diethanolamine (DEA), or methyl diethanolamine (MDEA) [3]. However, this process is less preferred because large volumes of the absorber are required to increase the contact area between the gas and the aqueous solution, and the risk of equipment corrosion could be high. Also, enormous energy is required for absorbent regeneration, and plentiful wastes and sludges are produced from the process. Alternatively, CO_2 adsorption

* Corresponding author.
E-mail address: nirattisai.ra@wu.ac.th (N. Rakmak).

https://doi.org/10.1016/j.heliyon.2020.e04019
Received 13 December 2019; Received in revised form 28 January 2020; Accepted 14 May 2020

by solid adsorbents is more comfortable to handle without any corrosion problem [4,5].

Activated carbons are widely known as a material with a high capacity to adsorb CO_2 and can be produced from low-cost and abundant precursors such as biochar. Nowadays, researchers also revealed that activated carbon could capture CO_2 because it consists of a large surface area in which CO2 can be adsorbed. From literature, it was proven that activated carbons prepared from biochar having different surface areas and pore size distributions exhibited different CO_2 capture performance [6,7]. Researchers successfully developed different precursors from abundant waste materials, such as palm oil mill residues, by considering cost-effectiveness in activated carbon production. Thus, palm oil mill residues were selected as a precursor for biochar production by the pyrolysis process in this study. Production of biochar from biomass depends on the process parameters involved. Recent studies on biomass pyrolysis have revealed that the production of biochar depended on several factors like the biomass particle size, the pyrolysis temperature, the flow rate of the carrier gas, and other factors such as the reactor type and catalyst [8, 9]. Besides the biochar yield, different properties of biochar also have been obtained due to different process conditions like pyrolysis temperature, residence time, and particle size. For getting the maximum production yield of biochar efficiently, the process parameters of the pyrolysis of biomass must be optimized. Several previous works studied the effects of process parameters on the production yield of bio-oil. However, suitable conditions for biochar production from biomass by pyrolysis have been less reported for substantial applications.

Conventional methods for studying multivariable/multifactor experiments were usually maintained other factors involved at certain constant levels but did not describe the combined effect of all factors involved. For optimization of a multiple variables system, these techniques usually vary one factor at a time. They could not reveal the interaction or combined effects between the factors or the variables. These methods were time-consuming and also required several experiments to determine the optimum levels, which sometimes were unreliable. Nowadays, experimental design techniques are one of the statistical experimental design methods for employed in chemical process optimization. Moreover, these techniques help in understanding the interactions among the optimizing parameters. A more popular technique in the recently is Response surface methodology (RSM). RSM is very effective for designing chemical processes, analyzing the process results, and optimizing the multivariable effect for the prediction of response output [10]. Box-Behnken design (BBD) of the RSM is widely used for design and optimization purposes of achieving better optimization output with the minimum number of experiments. Moreover, it explains the interactions between the parameters on the processes. This technique not only analyzes the influence of independent variables but also creates a second-order polynomial model describing the appropriate quantity of process [11].

This work aims to show the conversion of palm oil mill residues (namely, palm kernel shells, empty palm fruit bunches, and oil palm fibers) to biochar by the pyrolysis process and to study CO_2 adsorption on the biochar. Firstly, the suitable conditions of biochar production from the residues were sought by two series of experiments that were conducted in a pyrolysis-fixed bed reactor surrounded by a nitrogen atmosphere. RSM with BBD, a design of experimental techniques, was used to perform the experiments at five-factor levels with concern on optimization criterion. Three operating factors, namely: pyrolysis temperature, nitrogen (N_2) gas flow rate, and biomass particle size, were set as independent variables. By using RSM, the interaction of possible influencing process parameters on biochar yield can be evaluated. Contour and 3D response surfaces plots were used to indicate the region of the optimum condition. Secondly, the application of biochar for CO_2 capture was illustrated by the experiment using a fixed bed reactor to determine the CO_2 adsorption capacity of the biochar.

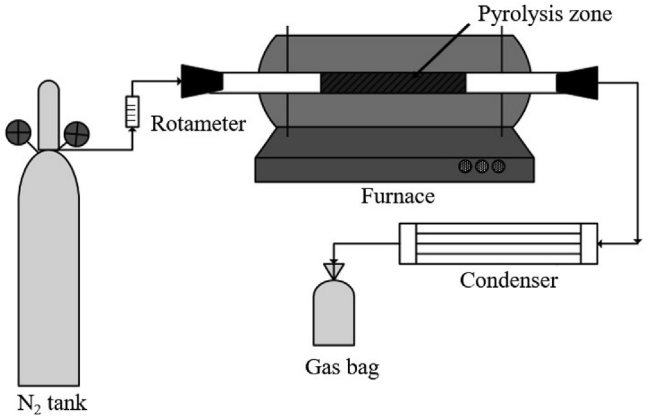

Figure 1. The schematic diagram of the apparatus for the fixed bed pyrolysis process.

2. Material and methods

2.1. Material

Biomass (palm oil mill residues) including palm kernel shells (obtained from the crushing of palm nuts in palm oil mills), empty palm fruit bunches (obtained after separating the fruits from sterilized fresh fruit bunches), and oil palm fibers (obtained after the crude palm oil was separated from the sterilized fruit through a screw-press) were collected from a palm oil mill factory (Palm D Srinakhon Company) in Nakhon Si Thammarat, Thailand. The collected biomass was usually dirty and contained moisture higher than 4 wt%. Therefore, preliminary preparation of the residues by mechanical and physical processing was required before they were used in the pyrolysis process. They were rinsed with sufficient water to eliminate any dirties and dried in an oven for 24 h. After that, palm oil mill residues were crushed and sieved to obtain a range of particle sizes, including sieve sizes of 300 μm, 600 μm, and 1,180 μm. Then, the sieved particles were kept in a desiccator to eliminate the remaining moisture for the next use.

2.2. Production and characterization of biochar

Biochar production from the palm oil mill residues was carried out in a laboratory-scale quartz-fixed bed reactor. The schematic diagram of the apparatus for the fixed bed pyrolysis process is shown in Figure 1. The reactor (90 cm in length and 30 mm in inner diameter) filled with 20 g of biomass was placed in the electric furnace. N_2 gas was flown from the left inlet to the right outlet of the reactor. The flow of N_2 washed out the air from the reactor and permitted the pyrolysis reaction to occur under anaerobic conditions. The N_2 gas carried vapors and gases produced from the pyrolysis of the biomass by the right outlet. The gas mixture passed through the condenser to keep in a liquid form. The biochar obtained from the pyrolysis process was collected after completing the pyrolysis reaction. The condenser collected the pyrolysis oil. The non-condensable gases were collected in a gasbag. The biochar produced was stored in a desiccator until all analyses were completed.

The yield of biochar can be calculated using Eq. (1).

$$\text{Biochar yield} = \frac{\text{the amount of biochar collected for a certain batch}}{\text{total amount of biomass in that batch}} \times 100 \quad (1)$$

Proximate analyses of biochar were performed using a thermogravimetric analyzer. Chemical compositions of the residual samples were assayed using the elemental CHNS/O analyzer to determine the

Table 1. Independent variables and their levels for experimental BBD used in the pyrolysis process.

Independent Variables	Symbol	Coded variable levels		
		-1	0	1
Pyrolysis temperature (°C)	X_1	450	500	550
The flow rate of N_2 (L/min)	X_2	1.50	2.00	2.50
Biomass particle size (μm)	X_3	300	600	1,180

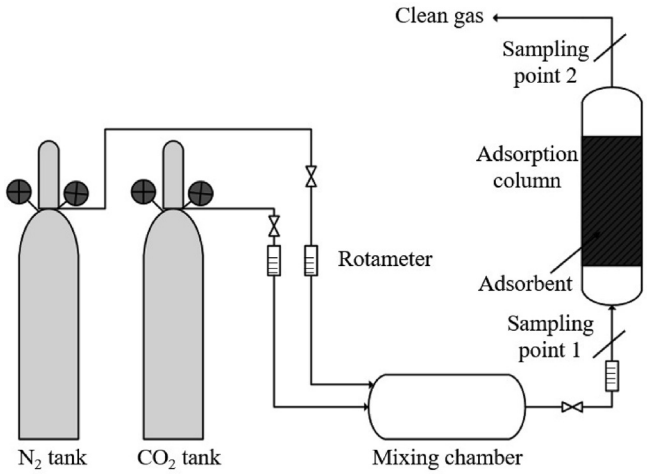

Figure 2. Schematic diagram of a fixed bed CO_2 adsorption system.

containing of chemical elements, including carbon (C), hydrogen (H), nitrogen (N), sulphur (S), and oxygen (O). Fourier Transform Infrared (FTIR) analysis was carried out with wavenumbers ranging from 400 cm^{-1} to 4,000 cm^{-1}. The surface area of each biochar sample was calculated from the Brunauer-Emmett-Teller (BET). Microscopic analysis was performed using a scanning electron microscope (SEM).

2.3. Experimental design

Two series of experiments were carried out. The first experiment was to study the effect of the residue types for biochar production. Three different types of palm oil mill residues (300 μm sieved size of 20 g of biomass), including palm kernel shells, empty palm fruit bunches, and oil palm fibers, were pyrolyzed at 500 °C with 2 L/min of N_2 flow rate for 60 min.

The second experiment was to obtain an optimal condition for biochar production by the pyrolysis process. RSM based on BBD was applied to design and optimize the production of biochar. The total design variables and the output responses at different operation parameters of biochar production were performed using the BBD. Three independent variables, including the pyrolysis temperatures (X_1) of 450 °C–550 °C, N_2 flow rates (X_2) of 1.5 L/min to 2.5 L/min, and biomass particle sizes (X_3) of 300 μm to 1,180 μm, were studied. Independent variables and their levels for experimental BBD are shown in Table 1.

The biochar yield was taken as the response. The total run numbers of the three factors by BBD (as provided in Table 3) with triplication at the designing center for assessing the pure error. The experimental sequences were conducted randomly. A replicate set of experiments was performed to evaluate the prediction errors. Experimental data were fitted to the second-order polynomial model as shown in Eq. (2),

$$Y_i = b_0 + \sum_{i=1}^{n} b_i x_i + \sum_{i=1}^{n} b_{ii} x_{ii}^2 + \sum_{i=1}^{n-1} \ldots \sum_{j=i+1}^{n} b_{ij} x_i x_j \quad (2)$$

where Y_i is the predicted response, n is the total number of factors or variables, b_0 is a constant, b_i is the linear coefficient, b_{ij} is the interactive coefficient, b_{ii} is the quadratic coefficient, and x_i to x_j are the coded values of the independent variables.

The optimization of the parameters was performed using biochar yield as the objective function. The statistical analysis of the model was represented by the analysis of variance (ANOVA) at a significance level of 0.05. ANOVA was not only used to check the model validity but also used to signify the relationship between the model and actual results. The fitness of the models was assessed from the coefficient of determination (R^2), and the adjusted R^2 value [12].

2.4. CO_2 adsorption

CO_2 adsorption experiments were conducted in a laboratory-scale fixed bed system. The schematic diagram of the generation of synthesized air waste (a mixture of pure CO_2 and N_2 gases) and the adsorption system are depicted in Figure 2.

Two sets of volumetric flow meters were used for controlling the composition of gas mixture. The fixed-bed adsorption column was made from a glass tube with dimensions of 40 cm in height and 3 cm in diameter. Fiberglass was installed at the bottom of the column to support the adsorbents. The concentration of CO_2 of the gas feed mixture was fixed by the composition controlling at 1,400 ppm. The flow rate of mixing gas was maintained at approximately 2.5 L/min. A biochar sample of 3.0 g was used to test the adsorbent's capacity in each experiment. The CO_2 adsorption was tested at atmospheric pressure and room temperature. A gas analyzer (MultiRAE Lite Gas Detector) was used to measure the CO_2 concentrations at the inlet and outlet gas streams every 10 s. When the difference between the two concentrations reached zero, the saturation of the adsorbents bed was reached. The tests on the capacity of adsorbents were performed at three replicates.

The percentage of CO_2 removal efficiency was calculated using Eq. (3).

$$CO_2 \text{ removal efficiency} = \frac{C_i - C_o}{C_i} \times 100 \quad (3)$$

where C_i and C_o are CO_2 concentrations (ppm) at the inlet and the outlet gas streams, respectively, of the adsorption column.

Table 2. Pyrolysis product from different types of palm oil mill residues.

Palm oil mill residues	Pyrolysis product yield (wt%)		
	Biochar	Bio-oil	Gas
Palm kernel shells	32.14	27.73	40.13
Empty palm fruit bunches	29.50	18.98	51.52
Oil palm fibers	26.28	11.55	62.17

Table 3. Corresponding between the experimental pattern using BBD method and the response values.

Standard run no.	Run	Coded values			Actual variables			Response values (wt%)		
		X_1	X_2	X_3	X_1	X_2	X_3	Biochar yield	Bio-oil yield	Gas yield
1	5	-1	0	-1	450	2.0	300	38.00	30.45	31.55
2	1	-1	-1	0	450	1.5	600	36.95	34.10	28.95
3	14	0	0	0	500	2.0	600	44.83	32.55	22.62
4	6	1	0	-1	550	2.0	300	42.30	29.60	28.10
5	8	1	0	1	550	2.0	1180	37.20	31.70	31.10
6	7	-1	0	1	450	2.0	1180	36.85	33.65	29.50
7	10	0	1	-1	500	2.5	300	39.60	29.40	31.00
8	15	0	0	0	500	2.0	600	44.77	32.55	22.68
9	11	0	-1	1	500	1.5	1180	36.60	33.30	30.10
10	4	1	1	0	550	2.5	600	41.31	32.70	25.99
11	12	0	1	1	500	2.5	1180	37.00	29.25	33.75
12	2	1	-1	0	550	1.5	600	42.65	33.45	23.90
13	3	-1	1	0	450	2.5	600	40.52	33.25	26.23
14	9	0	-1	-1	500	1.5	300	37.85	28.25	33.90
15	13	0	0	0	500	2.0	600	44.90	32.65	22.45

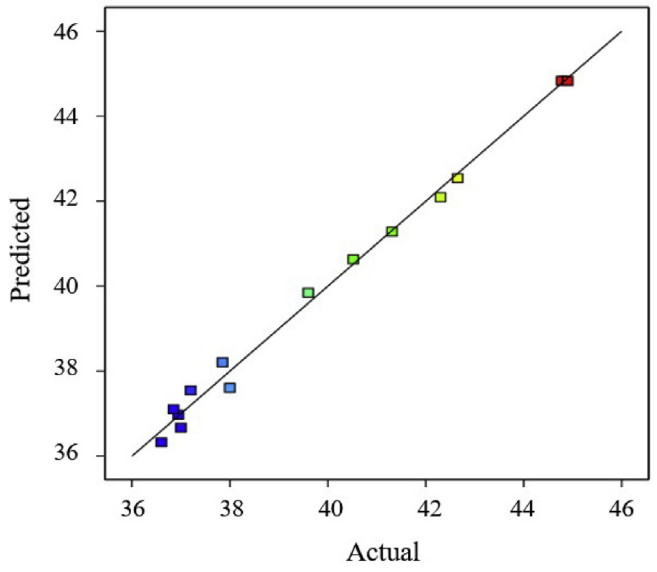

Figure 3. Predicted vs. actual experimental results for biochar production.

3. Results and discussion

3.1. Effect of the residue types on biochar production

The pyrolysis products from different types of palm oil mill residues are shown in Table 2. The optimum biochar yield of 32.14 wt% was obtained after pyrolysis of palm kernel shells at 500 °C with 2 L/min of N_2 flow rate for 60 min.

3.2. Box-Behnken design and statistical analysis

The complete set of experiments designed as coded levels, actual variables, and responses are shown in Table 3.

The statistical packaging software of Design Expert (Trial Version 11.0) was used to analyze the results. The ANOVA analysis of goodness-of-fit for the reduced quadratic model gave the coefficient of determination (R^2) and adjusted R^2 of 0.9994 and 0.9844, respectively. The reduced second-order polynomial model in the relation between the yield of the biochar product and selected three parameters was formulated from the multiple regression analysis of the experimental data. The equations obtained regarding coded factors are given in Eq. (4).

$$Y = 44.88 - 1.24X_1X_2 - 1.01X_1X_3 - 1.83X_1^2 - 2.65X_2^2 - 4.47X_3^2 \quad (4)$$

where Y is the yield of the biochar product. X_1, X_2, and X_3 represent the pyrolysis temperature, the flow rate of N_2, and the biomass particle size, respectively.

A comparison of predicted and actual experimental results for biochar production is depicted in Figure 3. It is seen in Figure 3, that the actual experimental data points lie close to the diagonal line, and the developed model can be used to predict biochar yield within the limits of the experimental factors. The predicted R^2 of 0.8918 reasonably agreed with the adjusted R^2 of 0.9844 since the difference is less than 0.1. The overall model prediction of the output in terms of the operation factors indicated that the model accurately predicted the production yield of biochar ($p < 0.01$).

To further understand the influence of the three variables on the biochar production by the pyrolysis process, the quadratic model was used to generate response surfaces and contours of biochar yields, as shown in Figure 4. Each surface plot or contour plot showed the interactive effects of two factors in experimental ranges of each factor, pinning one-factor constant at the center point of the designing box and varying the others. The ANOVA results showed that three factors (the pyrolysis temperature, the flow rate of N_2, and the particle size) have a significant influence on the response of biochar yield. The particle size had the most potent effect on the biochar yield. Furthermore, the biochar yield was significantly influenced by the quadratic effects from the three factors and the two interaction effects (the interaction between pyrolysis temperature and biomass particle size and the interaction between pyrolysis temperature and N_2 flow rate).

From the results in Figure 4, it was found that the yield of biochar products increased rapidly when the pyrolysis temperature increased from 450 °C up to approximately 530 °C. The maximum yield of biochar production was obtained at 525 °C. The further increase in temperature decreased the yield of biochar. Pyrolysis temperature is a crucial factor affecting the formation and volatilization of intermediate compounds. However, this volatilization process has indirect influences on porosity and surface areas. The yield of biochar reached the maximum when the flow rate of N_2 increased to approximately 2.0 L/min. It was anticipated that the increase of pyrolysis conversion influenced the yield of biochar corresponding to the amount of N_2 used. The results showed that the further increase in the flow rate of N_2 from the optimal flow rate gradually reduced the biochar yield at low pyrolysis temperatures. The flow

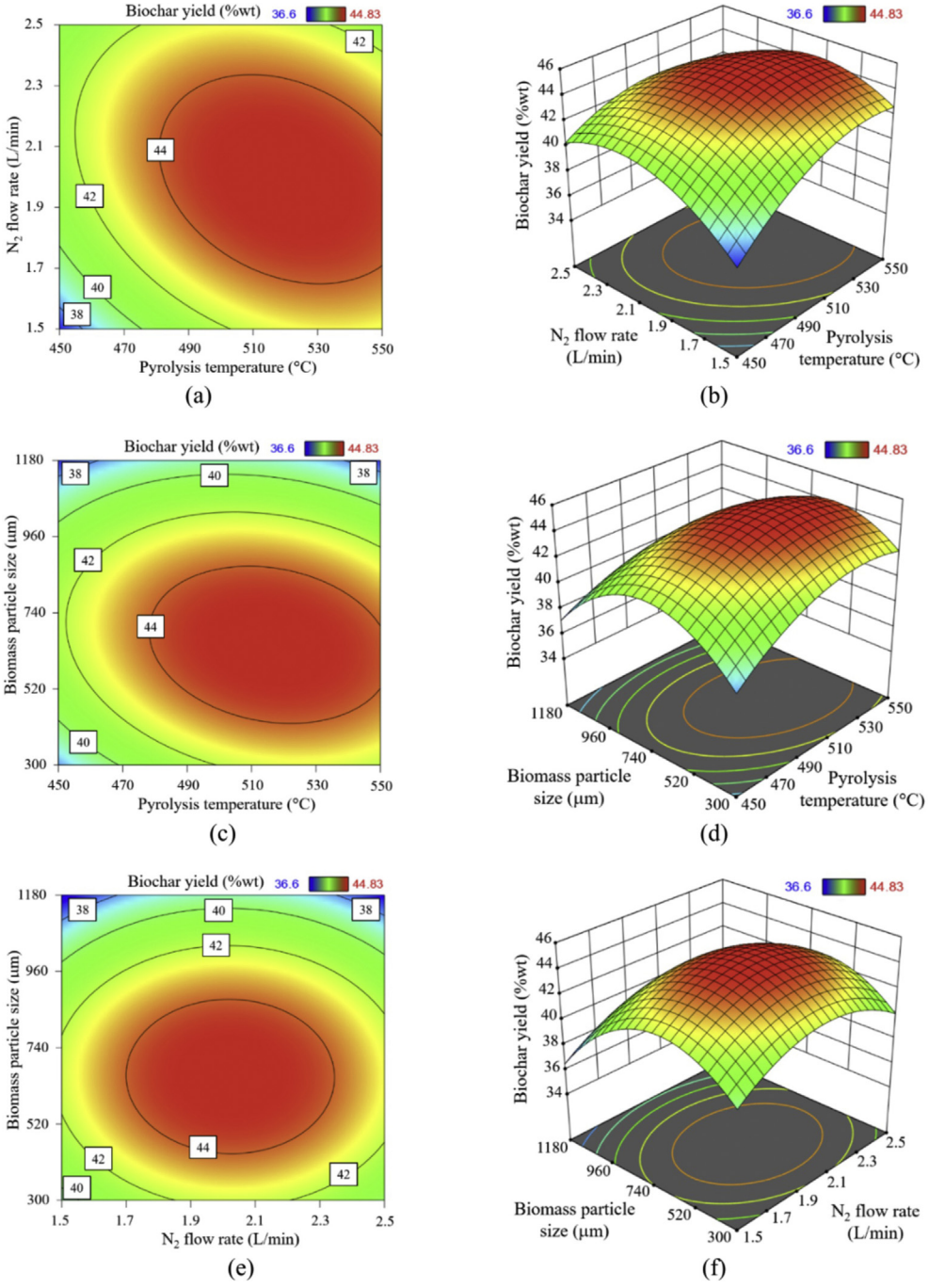

Figure 4. Contour plots and 3D surfaces by BBD for the interactive effects on the biochar yield: (a) contour plot for the N_2 flow rate and the pyrolysis temperature, (b) 3D surface for the N_2 flow rate and the pyrolysis temperature, (c) contour plot for the biomass particle size and the pyrolysis temperature, (d) 3D surface for the biomass particle size and the pyrolysis temperature, (e) contour plot for of the biomass particle size and the N_2 flow rate, and (f) 3D surface for the biomass particle size and the N_2 flow rate.

of N_2 gas could drive the vapors out of the reacting zone and resulting in a shortening of vapor residence time. Reducing the vapor residence time did not allow the volatile biomass components to initiate the re-polymerization process, and the volatiles was driven out rapidly, which consequently lowered the biochar yield [13].

Biomass particle size is one factor that could affect the pyrolysis process since it can control the rate of heat transfer in the biomass particle. Different product yields are commonly obtained when different particle sizes are used in the pyrolysis process. A larger particle size leads to lowering heat conduction inside the particle, and thus a longer heating time to reach the pyrolysis temperature is required. However, the tendency from experimental results showed that biochar yield was increased with the increase of the particle size from 300 µm to 750 µm. The further increase in the biomass particle size decreased the yield of biochar. This tendency was because sizes of particles too small (smaller than 750 µm) were overheated and induced to the following conversion of vapors into gas [13]. Lowering the heat transfer rate inside oversized particles was significantly pronounced when the particles were more extensive than 750 µm. Similar trends were reported in previous studies [14,15].

The optimization for the yield of biochar based on operating variables was performed using the response surface. The optimal condition for

Table 4. Proximate and ultimate analyses of different biomass.

Properties	Palm kernel shells	Empty palm fruit bunches	Oil palm fibers
Moisture content (wt%)	3	6	4
Proximate analysis			
Volatile fraction (wt%)	73	69	72
Fixed carbon (wt%)	20	22	19
Ash content (wt%)	4	3	5
Ultimate analysis (dry basis wt%)			
N	0.22 ± 0.003	0.600 ± 0.02	0.55 ± 0.01
C	48.60 ± 0.28	41.28 ± 0.19	45.58 ± 0.09
H	5.64 ± 0.04	5.22 ± 0.06	5.50 ± 0.03
S	Not detected	0.06 ± 0.002	0.07 ± 0.002
O	38.77 ± 0.31	38.99 ± 0.21	38.49 ± 0.32
Gross Heating Value (kcal/kg)	5,924.12 ± 34.05	5,181.30 ± 37.49	5,629.26 ± 17.12
Net Heating Value (kcal/kg)	5,634.96 ± 32.33	4,913.65 ± 34.26	5,347.29 ± 15.53

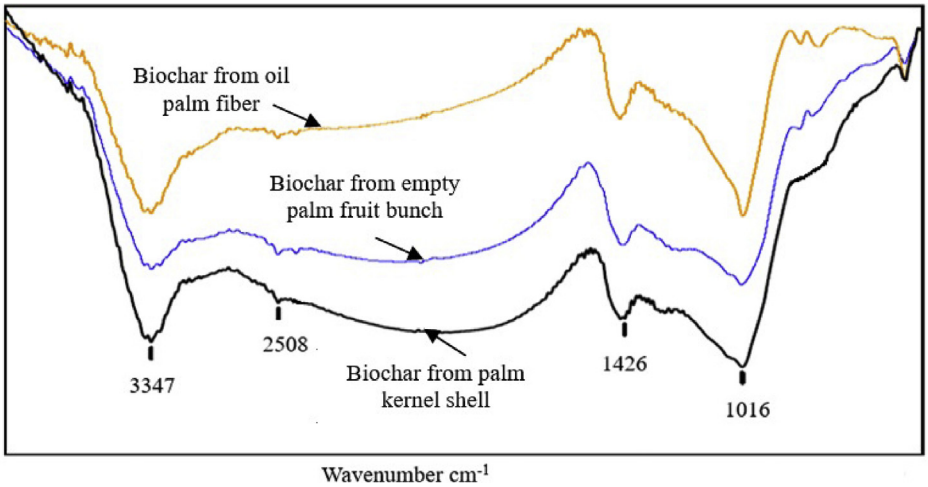

Figure 5. Fourier transform infrared (FTIR) spectra of biochar from palm kernel shells, empty palm fruit bunches, and oil palm fibers.

biochar production was obtained from the ANOVA analysis of the operation factors. The optimal yield of biochar (44.91 wt%) was at 525 °C, 2.0 L/min of N_2 flow rate, and particle size of 750 μm. The highest yield obtained from the pyrolysis of palm kernel shells at this condition gave higher yield than biochar yields reported in previous studies [16,17].

3.3. Characterization

3.3.1. Ultimate and proximate analyses

The properties, as well as ultimate and proximate analyses of palm oil mill residues, are summarized in Table 4.

Among the three types of residues, the palm kernel shells had the lowest moisture content. The volatiles, fixed carbon, and ash content were 73 wt%, 20 wt%, and 4 wt%, respectively. The palm kernel shells were analyzed to identify their chemical composition, which consisted of 0.22 ± 0.003 wt% of nitrogen, 48.60 ± 0.28 wt% of carbon, and 45.64 ± 0.04 wt% of hydrogen. Gross and net heating values of the palm kernel shells were 5,924.12 ± 34.05 kcal/kg and 5,634.96 ± 32.33 kcal/kg, respectively.

Table 5. Fourier transform infrared (FTIR) spectra of raw palm oil mill residues and their biochar.

Material	Wave numbers (cm^{-1})	Description
Raw palm kernel shells	3,347	Stretching of O–H in hydroxyl groups
	2,932	CH_2 symmetric stretching
	1,606	Strong aromatic ring stretch, aromatic C–O stretch, phenyl propanoic polymer, aromatic skeletal vibrations plus C=O stretch
	1,504	Semi-circle ring stretching in aromatic lignin
	1,452	C–H deformation (methyl and methylene) in hemicellulose and lignin
	1,240	Weak C–O stretching in hemicellulose
	1,032	C–O, C=C, and C–C–O vibrational stretching
Biochar from palm kernel shells	3,347	Stretching of O–H in hydroxyl groups and adsorbed water
	2,508	C–H stretching
	1,426	C=C stretching vibration of the aromatic ring
	1,016	Alcohol groups R–OH

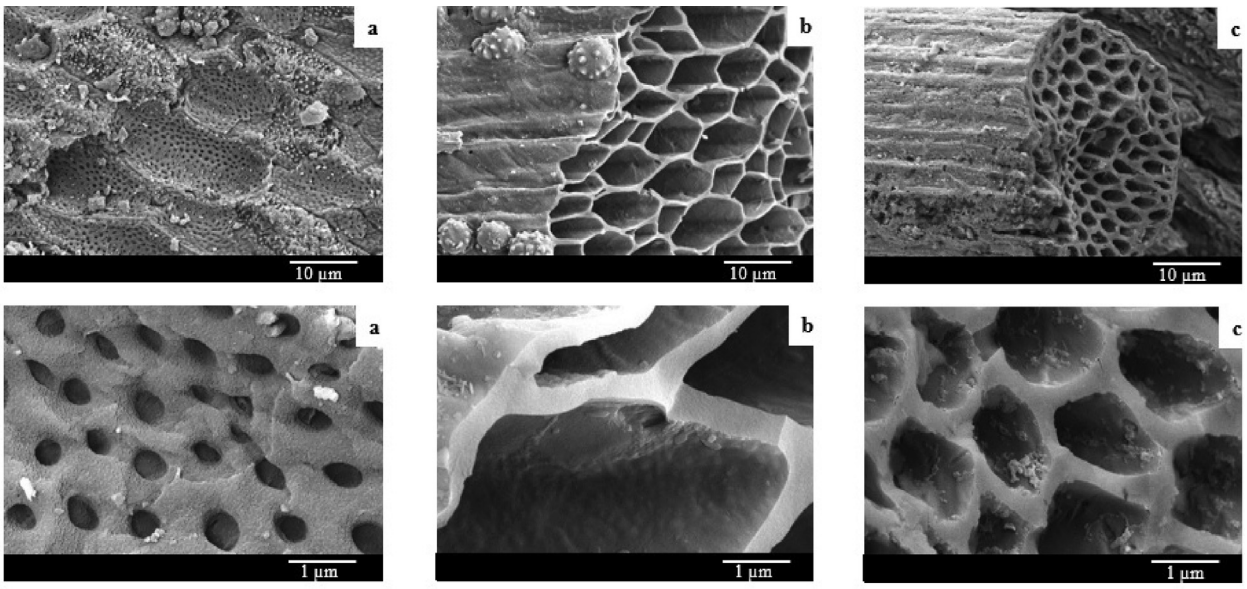

Figure 6. Morphology of biochar (a: biochar from palm kernel shells, b: biochar from empty palm fruit bunches, and c: biochar from oil palm fibers).

Table 6. BET surface area.

Sample		BET surface area (m^2/g)	References
Raw material	Palm kernel shells	0.7214	[7]
	Empty palm fruit bunches	2.0050	[19]
	Oil palm fibers	0.3805	[20]
Biochar product	Biochar from palm kernel shells	389.0200	This work
	Biochar from the empty palm fruit bunches	36.1136	This work
	Biochar from oil palm fibers	18.2876	This work

3.3.2. *Fourier Transform Infrared analysis*

FTIR spectra of all pyrolysis products obtained at 500 °C and 2 L/min of N_2 flow rate are illustrated in Figure 5. From the interpretation of the infrared transmittance spectrums, the functional group in the residual samples can be identified. These spectra allow the identification of structural changes in the surface functional group during the pyrolysis process. Active sites on the surface of the adsorbent should have base characteristics to enhance the adsorption of CO_2 from a gas mixture. Figure 5 showed that all of the biochar obtained from different raw materials at the same pyrolysis condition exhibited almost similar functional group bands. However, the spectra of the palm oil mill residues and their biochar had small differences in their functional group bands, as described in Table 5.

Based on the results in Figure 5 and Table 5, biochar from the palm kernel shells showed the most visible spectrum. A broad and robust adsorption peak appeared at 3,347 cm^{-1}, corresponding to the stretching of the O–H functional group. Biochar from the palm kernel shells showed similar functional groups, as reported in previous publications [16,18]. This sample also showed the C–H stretching at 2,508 cm^{-1}, the sharpest peak of C=C stretching at 1,426 cm^{-1}, and the R–OH functional group at 1,016 cm^{-1}.

3.3.3. *Surface area and Scanning Electron Microscopy (SEM) analysis*

The surface morphology of biochar products pyrolyzed from palm kernel shells, empty palm fruit bunches, and oil palm fibers at the same condition at 500 °C with 2 L/min of N_2 flow rate was examined using an SEM as shown in Figure 6. BET surface area of all raw materials used in this work and their biochar products pyrolyzed at this condition are summarized in Table 6. The BET surface area of biochar products was exceedingly higher than that of their raw materials. Generally, an adsorbent with a higher BET surface area will result in higher adsorption capacity. It can be stated that biochar obtained from the pyrolysis of the palm kernel shells gave the highest BET surface area (389.02 m^2/g) when compared with biochar from the empty palm fruit bunches (36.1136 m^2/g) and oil palm fibers (18.2876 m^2/g).

3.4. *CO_2 adsorption*

The application of biochar obtained from palm kernel shells by the pyrolysis condition at 500 °C and 2 L/min of N_2 flow rate was used for adsorption of CO_2 in the fixed bed reactor.

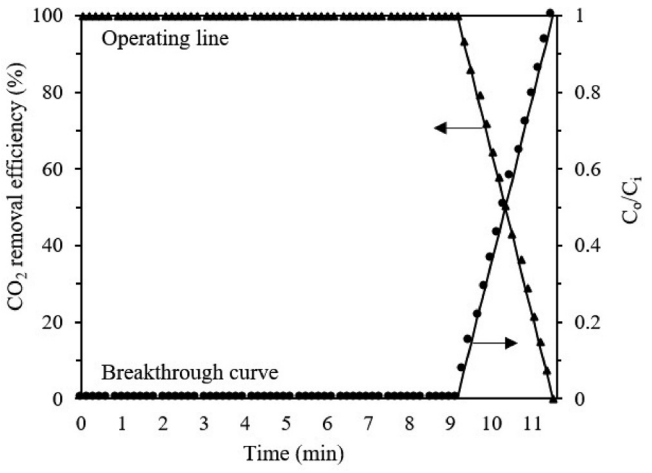

Figure 7. Operating line and breakthrough curve in CO_2 adsorption system by the biochar adsorbent.

Table 7. Breakthrough time and CO_2 adsorption capacity of biomass samples.

Adsorbent	Treatment method	CO_2 adsorption capacity (mmol/g)	References
Activated carbon from sea mango shells	Non-chemical treatment	0.219	[22]
Activated carbon from sea mango shells	Chemical/Deep eutectic solvent	0.223	[22]
Activated carbon from garlic peels	Chemical/KOH or HCl solution	1.3–4.2	[23]
Activated carbon from palm kernel shells	Chemical/Various concentrations and types of amines solution	1–1.5	[24]
Activated carbon from coconut shells	Non-chemical treatment	0.44	[25]
Biochar from palm kernel shells	Non-chemical treatment	0.46	This work

Figure 7 showed the operating line and the breakthrough at the test condition that the concentration of CO_2 was maintained at 1,400 ppm in N_2 gas. The flow rate of the gas mixture was controlled at approximately 2.5 L/min, and 3.0 g of adsorbent was used for this test. The CO_2 concentration in the outlet stream was ultimately zero until 9 min, which indicated a good potential of the biochar as the CO_2 adsorbent. This result agreed with the BET surface area in Table 6, where biochar from the palm kernel shells showed the highest value (389.02 m^2/g). The shape of the breakthrough curve clearly illustrated that CO_2 molecules easily penetrated through an absorbents bed having highly porous biochar and allowed a large amount of CO_2 to enter and be absorbed into the porous surface. Furthermore, it was anticipated that CO_2 molecules were adsorbed onto the pore surface of biochar due to a weak intermolecular cohesive force (physisorption) [21]. The CO_2 adsorption test was conducted to indicate the breakthrough time of each sample. Breakthrough time and the adsorption capacity of biomass samples in this study and previous studies are shown in Table 7.

Table 7 revealed that the CO_2 adsorption capacity of virgin carbonaceous materials could be improved by a surface modification using chemical treatment. Although those carbonaceous adsorbents have good potential for CO_2 adsorption, the production cost for synthesizing carbonaceous materials into adsorbents and further activation costs are high because of heat treatments at high temperatures. In the future, focusing on innovative research will be required to fill the gap between experimental data and the application use practically to initiate highly cost-effective production and activate processes of carbonaceous material adsorbents.

4. Conclusions

Palm kernel shells provided the highest biochar yield and the highest BET surface area when compared with empty palm fruit bunches and oil palm fibers used in the pyrolysis process at the same operating condition. The optimum condition for the pyrolysis of the palm kernel shells to yield biochar of 44.91 wt% was at 525 °C, 2.0 L/min of N_2 flow rate, and 750 μm of particle size. Biochar produced from the palm kernel shells was a suitable adsorbent for CO_2 adsorption. It may be considered as an alternative low production cost adsorbent to apply for CO_2 capture. The CO_2 adsorption capacity of the biochar obtained from the palm kernel shells was 0.46 mmol/g. Ongoing research would need to be conducted in order to develop a better adsorbent by using different chemical treatments on the biochar from palm kernel shells, which is possible to be an effective way to create a low-cost carbon for a high CO_2 uptake.

Declarations

Author contribution statement

Archw Promraksa: Analyzed and interpreted the data; Wrote the paper.

Nirattisai Rakmak: Conceived and designed the experiments; Performed the experiments; Analyzed and interpreted the data; Contributed reagents, materials, analysis tools or data; Wrote the paper.

Funding statement

The authors wish to acknowledge Walailak University (WU) for the research grant provided for this project. This research was partially supported by the New Strategic Research (P2P) Project (Phase 2), Walailak University, Thailand.

Competing interest statement

The authors declare no conflict of interest.

Additional information

No additional information is available for this paper.

References

[1] S. Prasertsan, P. Prasertsan, Biomass residues from palm oil mills in Thailand: an overview on quantity and potential usage, Biomass Bioenergy 11 (5) (1996) 387–395.
[2] H. Yang, R. Yan, H. Chen, D.H. Lee, D.T. Liang, C. Zheng, Mechanism of palm oil waste pyrolysis in a packed bed, Energy Fuels 20 (3) (2006) 1321–1328.
[3] F. Vega, M. Cano, S. Camino, B. Navarrete, J.A. Camino, Evaluation of the absorption performance of amine-based solvents for CO_2 capture based on partial oxy-combustion approach, Int. J. Greenhouse Gas Control 73 (2018) 95–103.
[4] C. Goel, H. Bhunia, P.K. Bajpai, Development of nitrogen enriched nanostructured carbon adsorbents for CO_2 capture, J. Environ. Manag. 162 (2015) 20–29.
[5] S. García, M.V. Gil, C.F. Martín, J.J. Pis, F. Rubiera, C. Pevida, Breakthrough adsorption study of a commercial activated carbon for pre-combustion CO_2 capture, Chem. Eng. J. 171 (2) (2011) 549–556.
[6] G. Skodras, I. Diamantopoulou, A. Zabaniotou, G. Stavropoulos, G.P. Sakellaropoulos, Enhanced mercury adsorption in activated carbons from biomass materials and waste tires, Fuel Process. Technol. 88 (8) (2007) 749–758.
[7] A.R. Hidayu, N. Muda, Preparation and characterization of impregnated activated carbon from palm kernel shell and coconut shell for CO_2 capture, Proc. Eng. 148 (2016) 106–113.
[8] W.T. Tsai, M.K. Lee, Y.M. Chang, Fast pyrolysis of rice straw, sugarcane bagasse and coconut shell in an induction-heating reactor, J. Anal. Appl. Pyrol. 76 (1-2) (2006) 230–237.
[9] B.B. Uzun, A.E. Pütün, E. Pütün, Fast pyrolysis of soybean cake: product yields and compositions, Bioresour. Technol. 97 (4) (2006) 569–576.
[10] M. Rajasimman, K. Murugaiyan, Sorption of Nickel by Hypnea Valentiae: application of response surface methodology, Int. Scholarly Sci. Res. Innovat. 5 (1) (2011) 7–12.
[11] C. Tian, Y. Chang, Z. Zhang, H. Wang, S. Xiao, C. Cui, M. Liu, Extraction technology, component analysis, antioxidant, antibacterial, analgesic and anti-inflammatory activities of flavonoids fraction from Tribulus terrestris L. leaves, Heliyon 5 (8) (2019), e02234.
[12] K. Mahalik, J.N. Sahu, A. Patwardhan, B.C. Meikap, Statistical modeling and optimization of hydrolysis of urea to generate ammonia for flue gas conditioning, J. Hazard Mater. 182 (1-3) (2010) 603–610.
[13] M. Tripathi, J.N. Sahu, P. Ganesan, Effect of process parameters on production of biochar from biomass waste through pyrolysis: a review, Renew. Sustain. Energy Rev. 55 (2016) 467–481.
[14] H.J. Park, J.-I. Dong, J.-K. Jeon, Y.-K. Park, K.-S. Yoo, S.-S. Kim, J. Kim, S. Kim, Effects of the operating parameters on the production of bio-oil in the fast pyrolysis of Japanese larch, Chem. Eng. J. 143 (1-3) (2008) 124–132.
[15] H.S. Choi, Y.S. Choi, H.C. Park, Fast pyrolysis characteristics of lignocellulosic biomass with varying reaction conditions, Renew. Energy 42 (2012) 131–135.
[16] U.D. Hamza, N.S. Nasri, N.S. Amin, J. Mohammed, H.M. Zain, Characteristics of oil palm shell biochar and activated carbon prepared at different carbonization times, Desalinat. Water Treat. 57 (17) (2015) 7999–8006.
[17] M. Mohd Hasan, R. Bachmann, S. Loh, S. Manroshan, S. Ong, Effect of pyrolysis temperature and time on properties of palm kernel shell-based biochar, IOP Conf. Ser. Mater. Sci. Eng. 548 (2019), 012020.

[18] S. Sumathi, S. Bhatia, K.T. Lee, A.R. Mohamed, Selection of best impregnated palm shell activated carbon (PSAC) for simultaneous removal of SO_2 and NOx, J. Hazard Mater. 176 (1-3) (2010) 1093–1096.
[19] A.R. Hidayu, N.F. Mohamad, S. Matali, A.S.A.K. Sharifah, Characterization of activated carbon prepared from oil palm empty fruit bunch using BET and FT-IR techniques, Proc. Eng. 68 (2013) 379–384.
[20] K.Y. Foo, B.H. Hameed, Microwave-assisted preparation of oil palm fiber activated carbon for methylene blue adsorption, Chem. Eng. J. 166 (2) (2011) 792–795.
[21] J.R. Richards, Control of Gaseous Emissions, Student Manual, APTI Course, third ed., 415, ICES Ltd, 2008, 4-1.
[22] N.Z. Zulkurnai, U.F. Md Ali, N. Ibrahim, N.S. Abdul Manan, Carbon dioxide (CO_2) adsorption by activated carbon functionalized with deep eutectic solvent (DES), IOP Conf. Ser. Mater. Sci. Eng. 206 (2017), 012001.
[23] G. Huang, Y. Liu, X. Wu, J. Cai, Activated carbons prepared by the KOH activation of a hydrochar from garlic peel and their CO_2 adsorption performance, N. Carbon Mater. 34 (3) (2019) 247–257.
[24] C.S. Lee, Y.L. Ong, M.K. Aroua, W.M.A.W. Daud, Impregnation of palm shell-based activated carbon with sterically hindered amines for CO_2 adsorption, Chem. Eng. J. 219 (2013) 558–564.
[25] F. Li, H. Yi, X. Tang, P. Ning, Q. Yu, Adsorption of carbon dioxide on coconut shell activated carbon, in: 2010 International Conference on Management and Service Science, 2010.